Academic Journal of Chemistry
ISSN(e): 2519-7045, ISSN(p): 2521-0211
Vol. 3, Issue. 10, pp: 88-100, 2018
URL: https://arpgweb.com/journal/journal/20
DOI: https://doi.org/10.32861/ajc.10.88.100

Academic Research Publishing Group

Original Research **Open Access**

Zirconium Phosphate/Fibrous Cerium Phosphate Nanocomposite Membrane Self Supported Benzimidazole, Its Co-Aniline, Co-Pyrrole and Co-Indole Polymerization Agent

S. K. Shakshooki *
Department of Chemistry, Faculty of Science, Tripoli University, Tripoli, Libya

F. A. Elakari
Department of Chemistry, Faculty of Science, Tripoli University, Tripoli, Libya

Aisha M. Shaabani
Department of Chemistry, Faculty of Science, Tripoli University, Tripoli, Libya

Abstract

Nanosized zirconium phosphate and nano fibrous cerium phosphate , $Zr(HPO_4)_2.H_2O$(nZrP) , $Ce(HPO_4)_2.2.9H_2O$ ($nCeP_f$), respectively, were prepared and characterized. Mixing slurry aqueous solution of (nZrP and $nCeP_f$) in 25:75 wt/wt% mixing ratios) , respectively, lead to formation of novel zirconium phosphate- fibrous cerium phosphate nanocomposite membrane, $[Zr(HPO_4)_2]_{0.25}[Ce(HPO_4)_2]_{0.75}.3.87H_2O$(nZrP-$nCeP_f$), was characterized. Zirconium phosphate-fibrous cerium phosphate/ polybenzimidazole-/polybenzimidazolee-co-polyaniline-/polybenzimidazole-co-polypyrrole-/polybenzimidazole-co-polyindole nanocomposite membranes were prepared via in-situ chemical oxidation polymerization of the benzimidazole, and its co-monomers in alcohol, that was promoted by the reduction of Ce(iv) ions present in the inorganic matrix of (nZrP-$nCeP_f$) nanocomposite membrane. A possible explanation is $nCeP_f$, present on the surface of composite membrane, is attacked by benzimidazole and its co-monomers , converted to cerium(III) orthophosphate($CePO_4$). The resultant materials were characterized by elemental (C,H,N) analysis , FT-IR, and scanning electron microscopy(SEM) .. SEM images of the resulting nanocomposites reveal a uniform distribution of the polybenzimidazole and its co-polymers on the inorganic matrix. From elemental (C,H,N) analysis the amount of organic material (PBI) present in (nZrP-$nCeP_f$)/PBI composite found to be = 5.7% in wt.. T.he amount of organic materials present in copolymers found to be for (nZrP-$nCeP_f$)/PBI-co-PANI (PBI = 9.33%, PANI= 13.32% in wt)., for (nZrP-$nCeP_f$) /PBI -co-PPy (PBI = 12.85%, PPy = 7.1% in wt) , and for (nZrP-$nCeP_f$) /PBI-co-PIn (PBI = 16.47% , PIn = 8.81% in wt).

Keywords: Zirconium phosphate; Cerium phosphate; Nanocomposite membrane; Self support polymerization; Benzimidazole-; Its co-aniline; Co-pyrrole and co-indole.

1. Introduction

Electronically conducting polymers have unique properties are the recent fields of increasing scientific and technical interest, offering the opportunity to synthesize a broad variety of promising new materials. They combine the chemical, electrochemical and mechanical properties of polymers with the electronic properties of metals and semiconductor, generated tremendous interest due to their potential applications in various fields such as rechargeable batteries, electrochromic display devices, separation membranes sensors and anticorrosive coatings on metals [1-10].

The properties of conducting polymers depend strongly on the doping level, protonation level , ion size of dopant, and water content [2, 3, 11, 12]. They exhibit wide range of electrical conductivity from semiconductors to metallic region by way of doping , They show enormous interesting properties like high electrical conductivity, environmental and chemical stability, low cost, easy prepared by chemical oxidative polymerization and electrochemical methods and fast reversible doping and de-doping, became materials of 21st century. .

Conducting polymers containing nitrogen atoms such as polyaniline, polypyrrole, polyindole , and polybenzimidazole and their substituted derivatives, belonging to the fused-ring family, have received increasing attention in various fields due to their unique physical , electrical and chemical properties [3, 6, 7, 9, 10]. These materials have an important influence on electrochromic device, sensors, catalysis, anticorrosion. Their electrical and electrochemical properties, owns advantages fairly good thermal stability show great promise for commercial applications [13-18]. However, polyindole and polybenzimidazole comparatively to polyaniline and poly pyrrole are less investigated.

Among conductive polymers, polyaniline (PANI) has attracted considerable attention, widely studied, because of its ease of preparation, low cost of monomer, good environmental stability, good conductivity control through doping as well as a good control of oxidation level. All these properties give PANI the potential for wide applications [15, 16, 18-20]. It can effectively be used as opto-electronic sensors [21-24], conductive paints and

*Corresponding Author

adhesive [25-27]. PANI has also good power and energy density, so it has been analyzed for the development of new super capacitor materials [28-31].

Polypyrrole (PPy) also has attracted considerable attention, widely considered conducting polymer and the most used polymer in commercial application. It shows good long term stability of its electric conductivity [1, 4, 8, 14, 32-36].

Polyindole (PIn) is an electro active polymer, owns advantages especially fairly good thermal stability [37, 38]. Polyindole can be obtained from chemical, electrochemical and interfacial polymerization of indole [37, 38]. Its electrical and electrochemical properties show great promise for commercial applications [39, 40]. Some studies shows polyindole has similar properties like polyaniline, based on their high conductance and good environmental stability [41, 42].

Polybenzimidazole(PBI) mainly was prepared from organic synthesis method , high performance polymer with high thermal stability, high conducting properties when doped. The preparation of PBI can be achieved by condensation reaction of diphenylisophthalate and 3,3',4,4'-tetraaminodiphenyl [43-49]. Recently we have reported synthesis of nanofibrous cerium(iv) Phosphate/ polybenzimidazole nanocomposite membrane [50].

Inorganic layered tetravalent metal phosphates nanomaterials are receiving great attention because of their size, structure, and possible biochemical applications [51, 52], that have been proven to be good carriers for organic polar molecules. These materials are good thermal stability and does not change on aging. Examples of these are zirconium phosphates. Taking advantage of the expandable of their layered.

Cerium phosphates have been studied for a long time as ion exchangers, their structures remains unknown until recently [53-55]. The reason is that, the composition, the structure and the degree of crystallinity of their precipitates results from reaction of solutions containing a Ce^{IV} salt is mixed with a solution of phosphoric acid of [(PO_4)/Ce(iv) ratio], strongly dependent on the experimental conditions such as rate and order of mixing of the solutions, stirring, temperature and digestion time, this also implemented on fibrous cerium phosphate [50, 56]. To date most of the work on fibrous cerium phosphate was carried out on its ion exchange [57], intercalation [58] and electrical conductance properties [59], on its poly(vinylalcohol) [60] and (polyvinyl chloride-based polyvinylalcohol) composites have been reported [61].

Nanoscaled tetravalent metal phosphates and their organic polymer composites comprise an important class of synthetic engineering. However; research in such area is still Terra incognita [62-65]. Nanotechnologies are at the center of numerous investigations and huge investments. Chemistry has anticipated for long the importance decreasing the size in the search of new properties of materials, and of materials structured at the nanosize in a number of applications relate to daily life. Organic-inorganic nanocomposite membranes have gained great attention recently [64, 66]. The composite material may combine the advantage of each material, for instance, flexibility, processability of polymers and the selectivity and thermal stability of the inorganic filler [63-67].

Recently we have reported [68-72] the preparation and characterization of composites fibrous cerium phosphate-tetravalent metal phosphates -, telluates, / polybenzimidazole- , polyindole and polyaniline nanocomposite membranes. Present study describes the preparation and characterization of novel conductive polymers nanocomposite membranes , the zirconium phosphate-fibrous cerium phosphate /polybenzimidazole, -/polybenzimidazole-co-polyaniline , -/ polybenzimidazole-co-polypyrrole, and / polybenzimidazole-co-polyindole nanocomposite membranes.,

2. Materials and Methods

2.1. Chemicals

$Ce(SO_4)_2.4H_2O$, $ZrOCl_2.8H_2O$, H_3PO_4(85 %) and benzimidazole of BDH, aniline (99.5%) of Mindex UK, pyrrole of Aldrich, indole of Reidel de-Haen. Other reagents used were of analytical grade.

2.2. Instruments Used For Characterization

X-Ray powder diffractometry Siemens D-500, using Ni-filtered CuKα (λ=1.54056Å), Thermogram C-MOM-Budapest, TG/DTA SIIExtra6000 TGA Perkin Elmer thermo gravimetric analyzer (TGA7)US, CHN-Elemental analyzer, Vario Elemental-German. Fourier Transform IR spectrometer, model FT/IR-6100, Scanning electron microscopy (SEM) Jeol SMJ Sm 5610 LV. Transmission electron microscopy) (TEM) Zeiss 10CR and pH Meter WGW 52.

2.3. Preparationof Nano Fibrous Cerium Phosphate($Ncep_f$)

300ml of 0.05M $CeSO_4.4H_2O$ in 0.5M H_2SO_4 solution were added drop wise to 300ml of 6M H_3PO_4 at 80°C with stirring. After complete addition the resultant material left to digest at that temperature for 4h.To that one liter of hot distilled water, (~60°C), was added with stirring for 1h. The resultant slurry aqueous solution of nanofibrous cerium phosphate was kept.

2.4. Preparation of Nano Zirconium Phosphate (Nzrp)

Nanosized zirconium phosphate , $Zr(HPO_4)_2.H_2O$(nZrP) , was obtained from refluxing 35g of wet gel zirconium phosphate in 2 molar H_3PO_4 for 50 hours.

2.5. Preparation Of Zirconium Phosphate-Fibrous Cerium Phosphate Nanocomposite Membrane(Nzrp-Ncep$_f$)

Slurry aqueous solution of 0.15g of $Zr(HPO_4)_2.H_2O$ (nZrP) in 20ml distilled water was added gradually to 150ml of slurry aqueous solution of fibrous cerium at 45°C , with stirring for 48h. The resultant product was filtered in Buchner funnel , washed with distilled water and dried in air.

2.6. Preparation of Nzrp-Ncep$_f$ / PBI Nanocomposite Membrane

0.132g of nZrP-nCeP$_f$ was immersed in 5ml 4% benzimidazole in ethanol at room temperature for 48h. Then the impregnated sheet was removed, washed with distilled water and ethanol and left to dry in air. The colour of the resultant product was beige.

2.7. Preparation of Nzrp-Ncep$_f$ / PBI-Co-Pani Nanocomposite Membrane

0.2g of nZrP-nCeP$_f$ composite sheet was immersed in a mixture of 10 ml 4% aniline and 10ml 4% benzimidazole in ethanol at room temperature for 48h.. The obtained composite membrane was washed with ethanol and left to dry in air. The colour of the resultant product was green.

2.8. Preparation of Nzrp-Ncep$_f$ / PBI-Co-Ppy Nanocomposite Membrane

0.2g of nZrP-nCeP$_f$ composite sheet was immersed in a mixture of 10ml 4% pyrrole and10ml 4% benzimidazole in ethanol, at room temperature for 48h. The obtained composite membrane was washed with ethanol and left to dry in air. The colour of the resultant product was green.

2.9. Preparation Of Nzrp-Ncep$_f$ / PBI-Co-Pin Nanocomposite Membrane

0.2g of nZrP-nCeP$_f$ composite sheet (0.2g) was immersed in a mixture of 10ml 4% indole and 10ml 4% benzimidazole in ethanol at room temperature for 48h. The obtained composite membrane was washed with ethanol and left to dry in air. The colour of the resultant product was brown.

3. Results and Discussion

Nanofibrous cerium phosphate membrane, $Ce(HPO_4)_2.\ 2.9H_2O$ (nCeP$_f$), was prepared, characterized by chemical, XRD, TGA, FT-IR, scanning electron microscopy (SEM) and transmission electron microscopy (TEM).

3.1. XRD of nCeP$_f$

XRD of (nCeP$_f$) is shown in Figure 1, withd_{001}=10.89Å.

Fig-1. XRD of nCeP$_f$

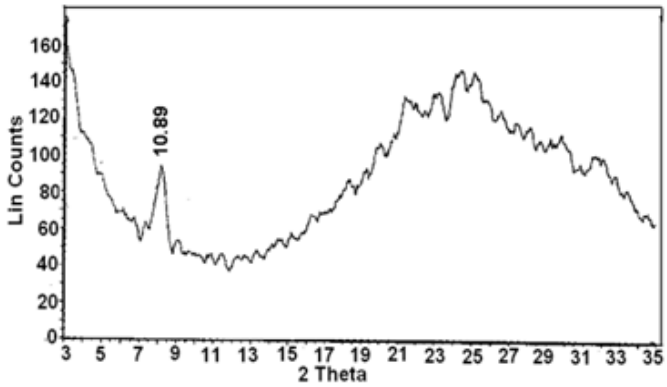

3.2. TGA of nCeP$_f$

Thermogram of (nCeP$_f$) is shown in Figure 2. The thermal decomposition occurs in continuous process, The thermal analysis was carried out at temperatures between 10-775°C, the final product was CeP_2O_7. Loss of water of hydration occurs between 60-200°C, followed by POH groups condensation. The total weight loss found to be equal to 19.09%.

Fig-2.TGA of $nCeP_f$

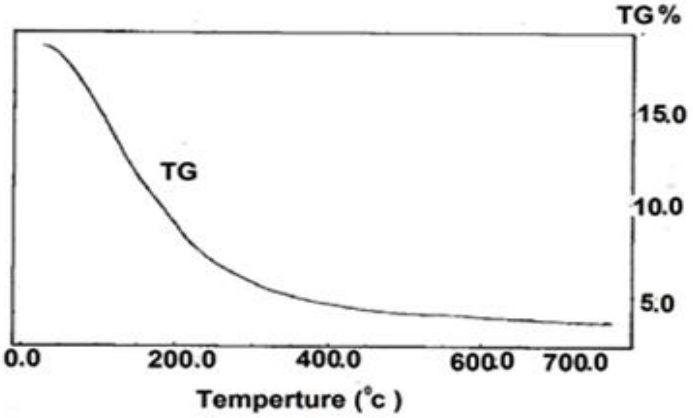

3.3. FT-IR of $nCeP_f$

Figure 3 shows FT-IR spectrum of fibrous $Ce(HPO_4)_2.2.9H_2O$, with a trend similar to that of M(IV) phosphates. It consists of broad band centered at $3350cm^{-1}$ is due to OH groups symmetric stretching of H_2O , small sharp band at $1628cm^{-1}$ is related to H-O-H bending , and sharp broad band centered at $1045cm^{-1}$ is corresponds to phosphate groups vibration The bands at the region 630-450 cm^{-1} are ascribe the presence of $\delta(PO_4)$.

Fig-3. FT-IR spectra of $nCeP_f$

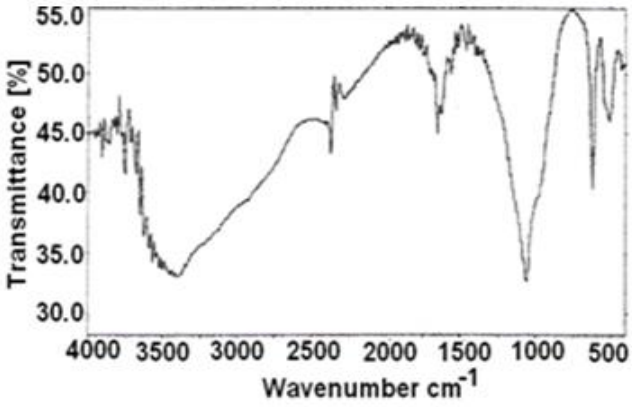

3.4. SEM of $nCeP_f$

SEM morphology image of the nanosized fibrous cerium phosphate ($nCeP_f$) is shown in Figure 4. The photograph shows its average size is ~20.5 nm.

Fig.4. SEM morphology image of $nCeP_f$.

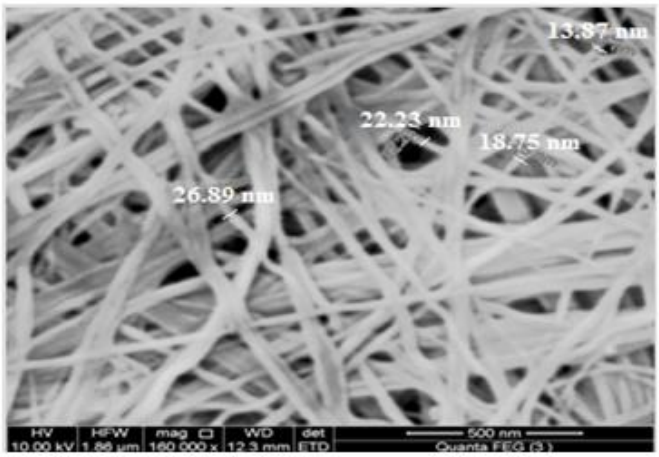

3.5. TEM of $nCeP_f$

Transmission electron microscopy image(TEM) of the nanosized fibrous cerium phosphate(2% in wt in PVA) , is shown in Figure 5. Its average size found to be ~15nm.

Fig.5. TEM image of $nCeP_f$.

3.6. Ion Exchange Capacity of Ncep$_f$

The ion exchange capacity of nanosized fibrous cerium(iv) phosphate , $Ce(HPO_4)_2.2.9H_2O$, and found to be equal to 5.21 meq/g.

Novel nanosized zirconium phosphate,$Zr(HPO_4)_2.H_2O$(nZrP), was prepared and characterized by XRD, TGA, FT-IR SEM and TEM.

3.7. XRD of nZrP

Figure 6 shows XRD of nanosized zirconium phosphate , its x-ray diffraction pattern Found to be similar to pellicular $Zr(HPO_4)_2.H_2O$. its $d_{001} = 7.65$ Å.

Fig-6. XRD of nZrP.3.8.SEM of nZrP.

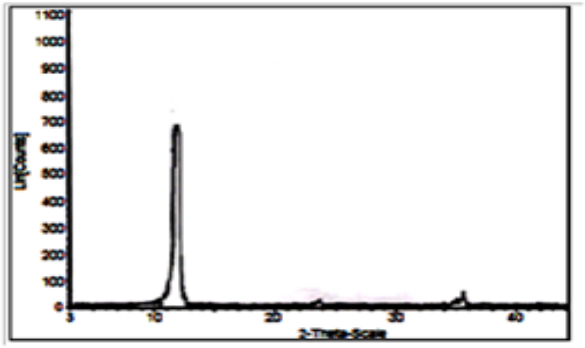

3.8. SEM of nZrP

SEM morphology image of the nanosized zirconium phosphate is shown in Figure 7. The photograph shows its average size in the range 48nm. Its interlayer distance (d_{001}) found to be equal to7.65Å.

Fig-7. SEM morphology image of nZrP.

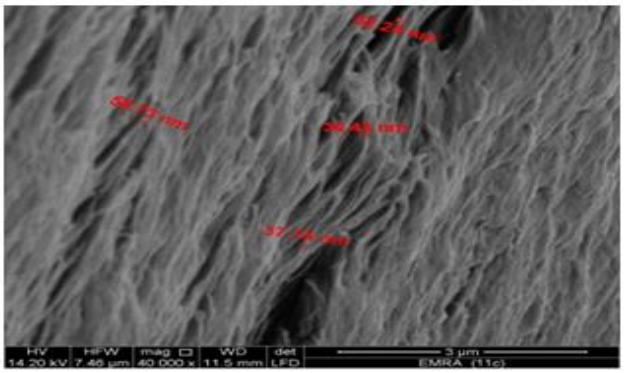

3.9. TEM of nZrP

Transmission electron microscopy image (TEM) of the nanosized zirconium phosphate is shown in Figure 8.The photograph shows its average size is ~85.7nm.

Fig-8. TEM morphology image of nZrP.

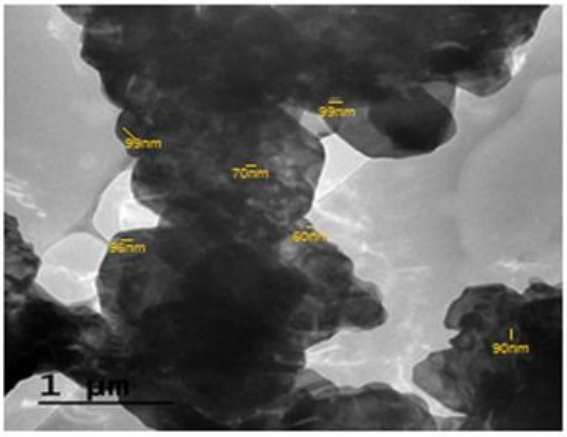

3.10. FT-IR of nZrP

The FT-IR spectrum are a key tool to detect the presence of water molecules as well as to investigate the H-bonds structure different forms with very different structures. Structures of the sample morphology in the FT-IR analysis allows understanding the structural changes involved in phase transition, proton exchange and hydration–dehydration process.

Figure 9 shows FT-IR spectrum of nZrP , consists of broad band centered at ~ 3250 cm^{-1} The two sharp side bands at 3590 and 3500 cm^{-1}, represent good crystallinity, include range of broad band, were attributed to symmetric asymmetric vibration of hydroxyl groups of water of crystallization. Sharp band at~ 1600 cm^{-1}, assigned for H-O-H bending .The broad band, with two small sharp band at 1250, 965 cm^{-1} with maxima at ~1040 cm^{-1} , is characteristic of the vibration of orthophosphate groups. The bands at the region 600- ~400 $cm^{-1}$are ascribe the presence of $\delta(PO_4)$.

Fig-9. FT-IR spectrum of nZrP.

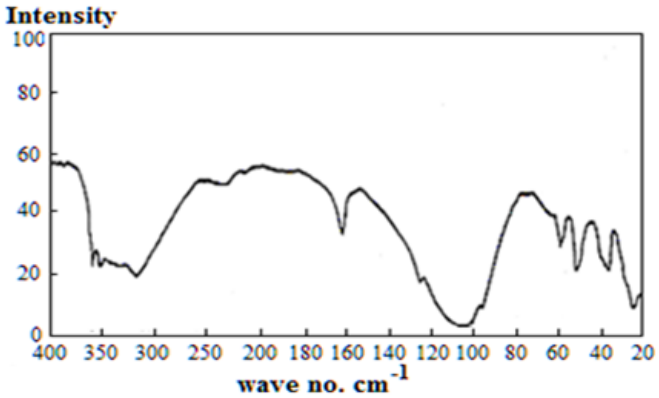

3.11. Ion Exchange Capacity of nZrP

The ion exchange capacity of nanosized zirconium phosphate found to be equal to 6.66 meq/g.

Zirconium phosphate fibrous cerium phosphate nanocomposite membrane was prepared and characterized by XRD, TGA and SEM.

3.12. XRD of nZrP-nCeP$_f$ Nanocomposite Membrane

X-ray diffraction of nanocomposite membrane, $[Zr(HPO_4)_2]_{0.25}[Ce(HPO_4)_2]_{0.75}$.$3.87H_2O$, Figure 10 shows two major peaks equal to 11.31Å and 7.81Å which are related to the interlayer distance of their parent materials which shows the formation of the composite. The first d value concern $nCeP_f$ the second one is related to nZrP.

Fig-10. XRD of nZrP- $nCeP_f$ nanocomposite membrane

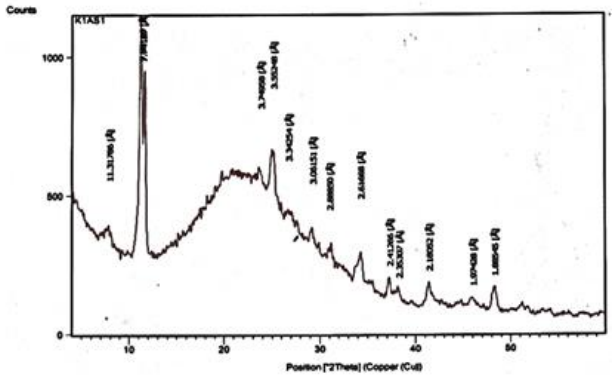

3.13. TGA of nZrP-$nCeP_f$ Nanocomposite Membrane

Thermogram of $[Zr(HPO_4)_2]_{0.25}[Ce(HPO_4)_2]_{0.75}.3.87H_2O$ is shown in Figure 11. The thermal analysis found to occur in three stages. The first stage is related to the loss of water of hydration between 75-240°C, followed by POH groups condensation up to 800°C. The total weight loss found to be equal to 20.1%. The final product was $[Zr_{0.25}\text{-}CeP_{0.75}]P_2O_7$ The thermogra is accomponed with four endothermic peaks.

Fig-11. TGA/DTA of nZrP-$nCeP_f$ nanocomposite membrane.

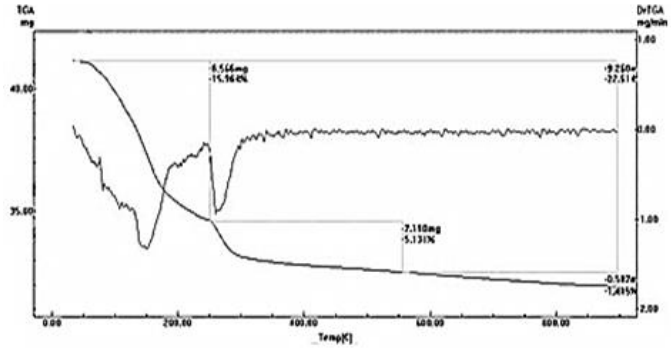

3.14. SEM of nZrP-$nCeP_f$ Nanocomposite Membrane

Figure 12 shows that the surface morphology of nanocomposite membrane $[Zr(HPO_4)_2]_{0.25}[Ce(HPO_4)_2]_{0.75}.3.87H_2O$ is totally different from their individual inorganic components. The morphology image reveal a uniform distribution of nZrP over and between fibrous cerium phosphate matrix.

Fig-12. SEM morphology image of nZrP-nCePf nanocomposite

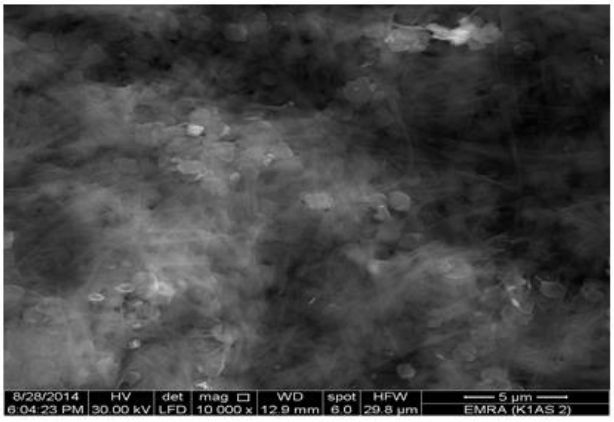

Novel polybenzimidazole and its co-polyaniline, co-polypyrrole and co-polyindole nanocomposites were prepared and investigated. Self-supported sheet of zirconium phosphate- fibrous cerium phosphate nanocomposite membrane, $[Zr(HPO_4)_2]_{0.25}$ $[Ce(HPO_4)2]_{0.75}$ $.3.87H_2O$ was used as polymerizing agent. The resultant nanocomposite membranes were characterized by elemental (C, H, N) analysis , FT-IR spectroscopy and SEM.

3.15. (nZrP-nCePf)/Polybenzimidazole Nanocomposite Membrane

It was found that when $[Zr(HPO_4)_2]_{0.25}[Ce(HPO_4)_2]_{0.75}.$ $3.87H_2O$ was immersed in ethanol solution of benzimidazole the colour of self supported sheet gradually changes with time to beige colour. From elemental (C, H, N) analysis, the amount of PBI present in the (nZrP-nCePf)/polybenzimidazole nanocomposite membrane was 5.7 % in wt.

3.15.1. FT-IR Spectra of nZrP-nCeP$_f$ / PBI Composite

FT-IR spectrum of nZrP-nCeP$_f$ / PBI composite is shown in Figure 13 , consist of broad band centered around ~ 3435cm^{-1}, is due to OH groups symmetric stretching of H_2O super imposed with the N–H stretching of aromatic amines (expected at the range 3695.9-.3000cm^{-1}),. Small band around ~1628 cm^{-1} is related to H-O-H bending , and sharp broad band centered at 1000.cm^{-1} is corresponds to phosphate groups vibration. Small bands at ~ 2924 , 2856cm^{-1} corresponds to C-H bonds, The presence of two bands in the range of 1600-1300 cm^{-1} is assigned to the (C=C stretching vibration of quinoid ring), while the lower frequency mode at ~1100cm^{-1} depicts the presence of benzenoid rings . However the higher frequency vibration has a major contribution from the quinoid rings (C=C stretching vibration of quinoid ring), Thus FT-IR spectrum confirms the formation of polymerization.

Fig-13. FT-IR spectrum of (nZrP- nCeP$_f$)/PBI nanocomposite.

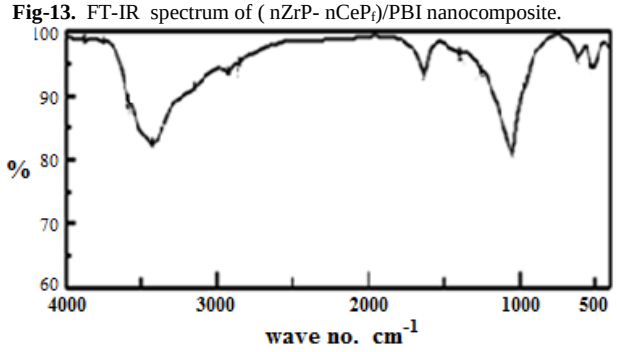

3.15.2. SEM of (nZrP-nCeP$_f$)/Polybenzimidazole Nanocomposite Membrane

Figure 14 shows SEM image for (nZrP-nCePf)/polybenzimidazole nanocomposite membrane, reveal a distribution of the polymer on the inorganic matrix

Fig-14. SEM of (nZrP-nCeP$_f$)/PBI nanocomposite.

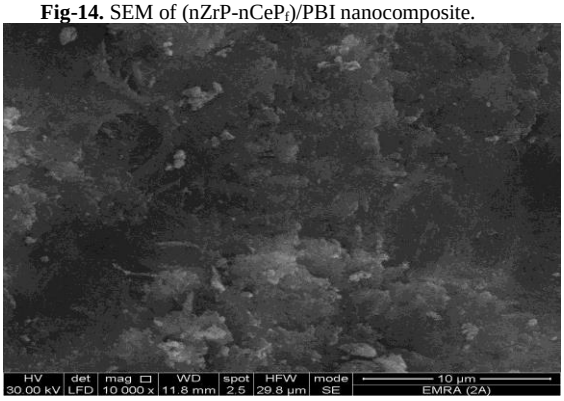

3.16. (nZrP-nCeP$_f$) / Polybenzimidazole-Co-Polyaniline/ -Polybenzimidazole-Co-Polypyrrole And / -Polybenzimidazole-Co-Polyindole Nanocomposite Membranes

On immersing of $[Zr(HPO_4)2]_{0.25}[Ce(HPO_4)_2]_{0.75}.3.87H_2O$ nanocomposite membrane in ethanol solution of benzimidazole-co-monomers (aniline, pyrrole and indole), respectively, the colour of the sheets gradually changes with time to green, green, and brown, respectively. From elemental (C,H,N) analysis of the amount of organic materials present in (nZrP-nCeP$_f$)/PBI-co-polymers were for / -co-PANI (PBI = 9.33%, PANI =13.32% in wt.), for /-co-PPy ,(PBI = 12.85%, PPy = 7.1% in wt.) and for /-co-PIn ,(PBI = 16.47% , PIn = 8.81% in wt.).

3.16.1. FT-IR of (nZrP-nCeP$_f$)/ Polybenzimidazole-Co-Polyaniline Nanocomposite

Figure 15 shows FT-IR spectrum of nZrP-nCeP$_f$ polybenzimidazole-co-polyaniline nanocomposites polybenzimidazole-co-polyaniline consists of broad band centered at 3400 cm^{-1}, due to the characteristic stretching vibration OH groups symmetric of H_2O, superimposed with that of N-H stretching of aromatic amines. Small bands at the range 2960-2865cm^{-1} could be attributed to N-H stretching. Bands in the region 1680-1600cm^{-1} are related to stretching C-C bonds characteristic of C-H (aromatic) stretching, C=C stretching. C-N stretching. The presence of bands in the range 1455–1373 cm^{-1} is assigned to the non-symmetric C_6 ring stretching modes and contribution from the quinoid rings, the presence of benzenoid units of polyaniline. However, the characteristic band for polybenzimidazole are found in the range 1487-1176cm^{-1}. Small sharp band at 1625 cm^{-1} is related to H-O-H bending. Sharp broad band centered at 1015 cm^{-1} is corresponds to phosphate groups vibration.

Fig-15. FT-IR of($nZrP_{M2}$-$nCeP_f$)/polybenzimidazole-co-polyaniline nanocomposite

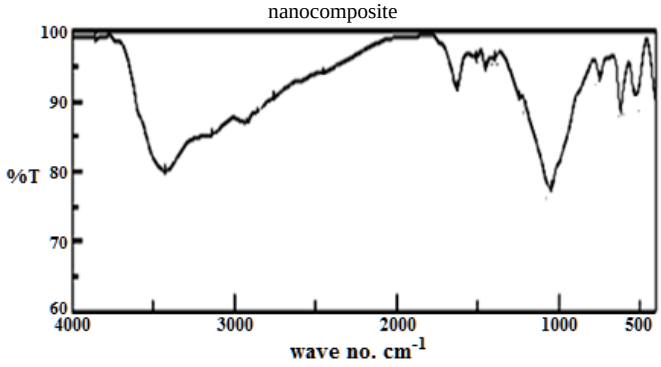

3.16.2. SEM of (nZrP-nCeP_f)/ Polybenzimidazole-Co-Polyaniline Nanocomposite

Figure 16 shows SEM image for (nZrP-nCePf)/polybenzimidazole-co-polyaniline nanocomposite membrane, reveal a distribution of the co-polymer on the inorganic matrix

Fig-16. SEM of ($nZrP_{M2}$-$nCeP_f$)/ polybenzimidazole-co-polyaniline nanocomposite.

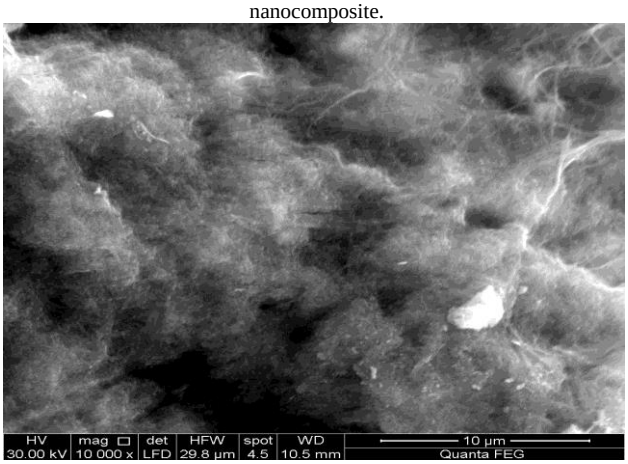

3.16.3. FT-IR of ($nZrP_{M2}$-nCeP_f)/ Polybenzimidzole-Co-Polypyrrole Nanocomposite

FT-IR spectrum of polybenzimidazole-co-polypyrrole nanocomposite copolymer is shown in Figure 17. A broad band cantered at 3400 cm^{-1}, due to the characteristic stretching vibration OH groups symmetric of H_2O, superimposed with that of N-H stretching of aromatic amines. Small bands at the range 2960-2865cm^{-1} could be attributed to N-H stretching. Bands in the region 1680-1600cm^{-1} are related to stretching C-C bonds characteristic of pyrrole unites C-H (aromatic) stretching, C=C stretching. C-N stretching (between two indole units), are in the region 1570-1370cm^{-1} .The presence of bands in the range 1455–1373 cm^{-1} is assigned to the non-symmetric C6 ring stretching modes and contribution from the quinoid rings, the presence of benzenoid units. However, the characteristic band for polybenzimidazole are found in the range of 1487-1176cm^{-1}. Small sharp band at 1625 cm^{-1} is related to H-O-H bending, Sharp broad band centered at 1040 cm^{-1} is corresponds to phosphate groups vibration .

Fig-17. FT-IR of ($nZrP_{M2}$-$nCeP_f$)/ polybenzimidazole-co-polypyrrole nanocomposite

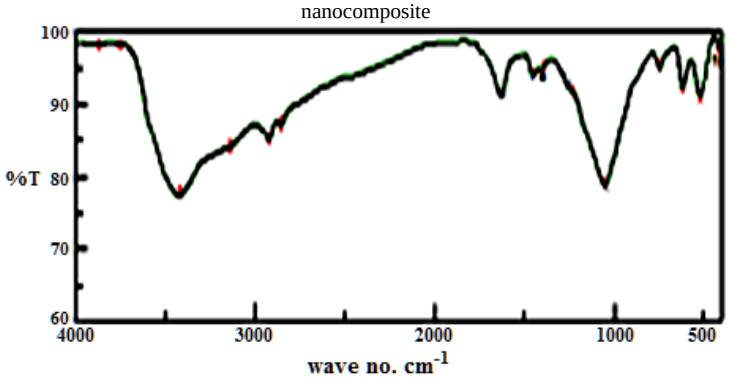

3.16.4. SEM of (nZrP-nCeP_f)/ Polybenzimidazole-Co-Polypyrrole Nanocomposite

Figure 18 shows SEM image for (nZrP-nCePf)/polybenzimidazole-co-polypyrrole nanocomposite membrane, reveal a distribution of the co-polymer on the inorganic matrix

Fig-18. SEM of (nZrP $_{M2}$-nCeP$_f$)/ polybenzimidazole-co-polypyrrole nanocomposite

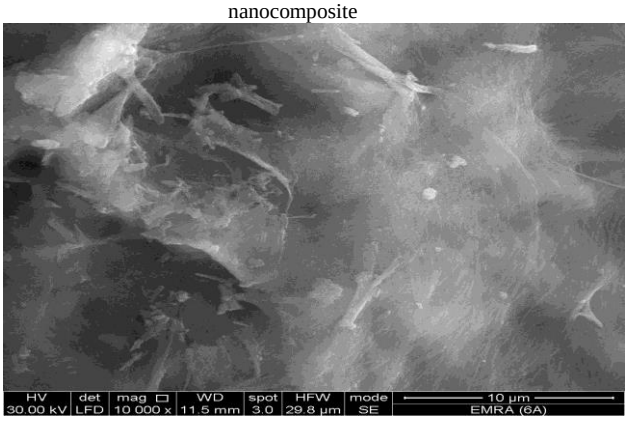

3.16.5. FT-IR of (nZrP$_{M2}$-nCeP$_f$)/ Polybenzimidazole–Co-Polyindole Nanocomposite

Figure 19 shows FT-IR spectrum of nZrP$_{M2}$.nCeP$_f$ / polybenzimidazole-co-polyindole nanocomposite membrane. A broad band cantered at 3400 cm^{-1}, due to the characteristic stretching vibration OH groups symmetric of H_2O, superimposed with that of N-H stretching of aromatic amines. Small bands at the range 2960-2865cm^{-1} could be attributed to N-H stretching. bands in the region 1680-1600cm^{-1} are related to stretching C-C bonds characteristic of pyrrole unites C-H (aromatic) stretching, C=C stretching. C-N stretching (between two indole units), are in the region 1570-1370cm^{-1} . The presence of bands in the range 1455–1373 cm^{-1} is assigned to the non-symmetric C6 ring stretching modes and contribution from the quinoid rings, the presence of benzenoid units of polyindole . However, the characteristic band for polybenzimidazole are found in the range of 1487-1176cm^{-1} . Small sharp band at 1625 cm^{-1} is related to H-O-H bending. Sharp broad band cantered at 1040 cm^{-1} is corresponds to phosphate groups vibration.

Fig- 19. FT-IR of (nZrP$_{M2}$-nCeP$_f$)/ polybenzimidazole-co-polyindole nanocomposite

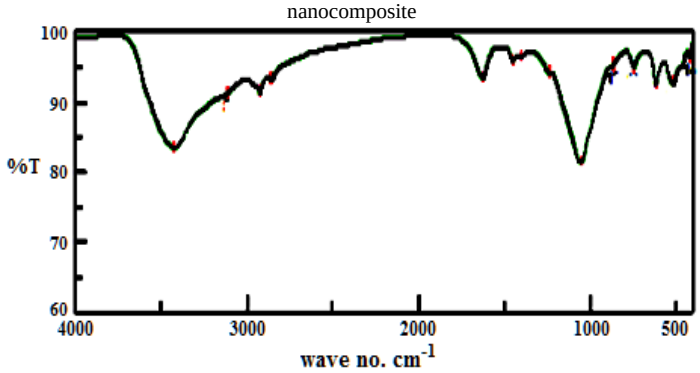

3.16.6. SEM of (nZrP-nCeP$_f$)/ polybenzimidazole-co-polyindole nanocomposite

Figure 21 shows SEM image for (nZrP-nCePf)/polybenzimidazole-co-polyindole nanocomposite membrane, reveal a distribution of the co-polymer on the inorganic matrix

Fig-20. SEM of (nZrP $_{M2}$-nCeP$_f$)/ -polybenzimidazole-co-polyindole nanocomposite

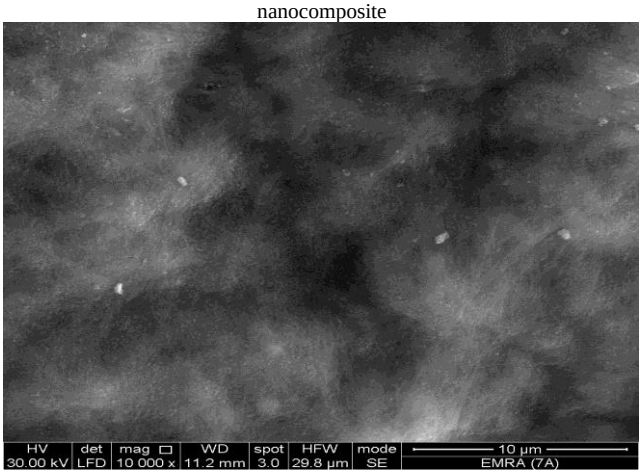

4. Conclusion

Nanosized zirconium phosphate and nanofibrous cerium phosphate , $Zr(HPO_4)_2.H_2O$(nZrP) , $Ce(HPO_4)_2.2.9H_2O$ ($nCeP_f$), respectively, were prepared and characterized. Mixing slurry aqueous solution of (nZrP and $nCeP_f$) in 25:75 wt/wt% mixing ratios , respectively, lead to formation of novel zirconium phosphate-fibrous cerium phosphate nanocomposite membrane, $[Zr(HPO_4)_2]_{0.25}[Ce(HPO_4)_2]_{0.75}.3.87H_2O$(nZrP-$nCeP_f$), and was characterized. Zirconium phosphate-fibrous cerium phosphate/ polybenzimidazole-/ polybenzimidazolee-co-polyaniline-/polybenzimidazole-co-polypyrrole-/ and polybenzimidazole-co-polyindolenanocomposite membranes were prepared via in-situ chemical oxidation of the benzimidazole, and its co-monomers that was promoted by the reduction of Ce(iv) ions present in the inorganic matrix of (nZrP-$nCeP_f$) nanocomposite membrane.

The presence of Ce(iv) ions allows redox reactions necessary to oxidative polymerization to occur. A possible explanation is that polymerization of BI and its co-monomers were promoted by the reduction of some of nCePf present in inorganic composite membrane (nZrP-$nCeP_f$), that attacked by BI , and its co-monomers, respectively, converted to cerium(III) orthophosphate ($CePO_4$).

The formulation of the resultant conducting polymers nanocomposites was supported by elemental(C,H,N) analysis, FT-IR spectra and SEM. Colour changes supports the formation of the resultant organic polymers composites . We suggest self doping occurred on polymerization, which is due to H^+ present in (ZrO_3POH) groups.

Beneficial properties of the resultant nanocomposites can be considered these composites as novel conducting inorganic-organic composites, ion exchangers, solid acid catalyst and as sensors.

Acknowledgements

To Department of Chemistry, Faculty of Science, University of Tripoli . Tripoli, Libya, for supporting of this research.

References

[1] Banerjee, S. and Tayagi, A. K., 2012. "Func-tional materials: Preparation, proscessing and applications." *Elsevier*,

[2] Freund, M. S. and Deore, B. A., 2007. *Self doped conducting polymers*. John Wiley and Sons.

[3] Heeger, A., 2001. "Semiconducting and metallic polymers: The fourth generation of poly-meric materials." *Reviews of Modern Phys.*, vol. 73, p. 681.

[4] Kucheldorf, H. R., Luken, O., and Swift, G., 2010. *Hand book of polymer synthesis*. 2nd ed. CRC Press.

[5] Lange, U., Roznyatovskaya, N. V., and Mirsky, V. M., 2008. "Conducting polymers in chemical sensors and arrays." *Analytica Chimica Acta*, vol. 614,

[6] MacDiarmid, A. G., 2001. "A novel role for organic polymers." *Angewandte Chemie Interna-tional Edition*, vol. 40, p. 2581.

[7] Nalwa, H. S., 1997. *Handbook of organic conductive molecules and polymers* vol. 2. UK: John Wiley, Chichester.

[8] Sapurina, I. Y. and Shishov, M. A., 2012. "New polymers for special applications, ailton de souza gomes."

[9] Skotheim, T. J. and Reynolds, J. R., 1997. *Hand-book of conducting polymers*. 3rd ed. USA: CRC Press, Boca Raton.

[10] Street, G. B. and Clarke, T. C., 1981. "Conducting polymers: A review of recent work." *IBM J. Res. Dev.*, vol. 25, pp. 51-57.

[11] Cai, Z., Grang, M., and Tang, Z., 2004. "Novel bat-tery using conducting polymers, And polyaniline." *J .of Mater. Sci.*, vol. 39, p. 4001.

[12] Ćirić-Marjanović, G., 2010. *Polyaniline nanostructures, in nanostructured conduc-tive polymers, eftekhari, a. Ed.* John Wiley & Sons, Ltd.

[13] Fajan, A. and Been, B., 2013. "Structural and optical properties of polyindole manganese oxide nanocomposite." *Indian J. of Adv. in Chem. Sci.*, vol. 2, pp. 95-96.

[14] Feng-Hao, H. F. H. and Wu, T. M., 2012. "In situ synthesis and characterization of conductive polypyrrole/graphene composites with im-proved solubility and conductivity." *Syn-thetic Metals.*, vol. 162, pp. 682-687.

[15] Green, A. G. and Woodhead, A. E., 1997. *J. Chem. Soc.*, vol. 1910, pp. 2388-2403.

[16] Sharma, A. K. and Sharma, Y., 2013. *J. Electrochem. Sci. Eng.*, vol. 3, pp. 47-56.

[17] Vernitskaya, T. V., Tat'yana, V. V., and Efimov, 1997. "Polypyrrole, A conducting polymer, Its syn-thesis, properties and applications." *Russ. Chem. Rev.*, pp. 66-443.

[18] Wang, C., Yu, H. C., and Chen , K., 2018. "Clip-like polyaniline nanofiber synthesized by an in-situ chemical oxidative polymerization and its strong electro rheological behavior." vol. 239, pp. 1-12.

[19] Magioli, M., Soares, B. G., Sirqueira, A. S., Rahaman, M., and Khastgir, D., 2012. *J. Appl. Polym. Sci.*, vol. 125, pp. 1476-1485.

[20] Rahaman, M., Nayak, L., Chaki, T. K., and Khastgir, D., 2012. *Adv. Sci. Lett.*, vol. 18, pp. 54-61.

[21] Bhadra, S., Chattopadhyay, S., Singha, N. K., and Khastgir, D., 2008. *J. Appl. Polym. Sci.*, vol. 108, pp. 57-64.

[22] Bhadra, S. and Khastgir, D., 2008. *Polym. Test.*, vol. 27, pp. 851-857.

[23] Bhadra, S., Khastgir, D., Singha, N. K., and Lee, J. H., 2009. *Prog. Polym. Sci.*, vol. 34, pp. 783-810.

[24] Rahaman, M., Chaki, T. K., and Khastgir, D., 2013. *J. Appl. Polym. Sci.*, vol. 128, pp. 161-168.

[25] Chiang, J. C. and MacDiarmid, A. G., 1986. *Synth. Met.*, vol. 13, pp. 193-205.
[26] Hualan, W., Qingli, H., Xujie, Y., Lude, L., and Xin, W., 2009. *Electrochem. Commun.*, vol. 11, pp. 1158-1161.
[27] Zheng, J. P., Cygan, P. J., and Jow, T. R., 1995. *J. Electro-chem. Soc.*, vol. 142, p. 2699.
[28] Burke, A. J., 2000. *J. Power Sources*, vol. 91, p. 37.
[29] Chandra, S., 2012. *Chem. Phys. Lett.*, vol. 2012, pp. 519-520
[30] Conway, B. E., 1999. *Electrochemical Super capac-itors*. New York: Kluwer-Plenum.
[31] Sopčić, S., Kraljić, R. M., and Mandić, Z., 2012. *J. Electrochem. Sci. Eng.*, vol. 2, pp. 41-52.
[32] Chitte, H. K., Shinde, G. N., Bhat, N. V., and Walunj, V. E., 2011. "Synthesis of polypyrrole using ferric chloride (fecl3) as oxidant together with some dopants for use in gas sensors." *Journal of Sensor Tech*, vol. 1, pp. 2161-1238.
[33] Ebrahim, S. M., Abd-ElLatif, M. M., Gad, A. M., and Soliman, M. M., 2010. "Cy-clic voltammetry and impedance studies of elec-trodeposited polypyrrole nanoparticles doped with 2-acrylamido-2-methyl-1-propanesulfonic acid sodium salt." *Thin Solid Films*, vol. 518, pp. 4100-4105.
[34] Hail, V. V. T., Hang, T. T., Xuan, H. T. T., Thi, N., Thom, N. T. P., Nguyen, T. N., Didier, D. T., and Thi, M. D. T., 2018. "Synthesis of silica/polypyrrole nanocomposites and applica-tion in corrosion protection of carbon steel." *J.of NanoSc. and Nanotech.*, vol. 18, pp. 4189-41957.
[35] Lee, J. K., Jeong, H., Lassarote, R., Lavall, R. L. A., Busnaina, A., Younglae, K. Y., Jung, Y. J., and Lee, H. Y., 2017. "Polypyrrole films with micro/nanosphere shapes for electrodes of high-performance supercapacitors." *ACS Appl. Mater. Interfaces*, vol. 9, pp. 33203-33211.
[36] Ermişn, N. and Tınkılıç, N., 2018. "Preparation of molecularly imprinted polypyrrole modified gold electrode for determination of tyrosine in biolog-ical samples." *Int. J. Electrochem. Sci.*, vol. 13, pp. 2286–2298.
[37] Billand, B., Maarouf, E., and Hamecant, E., 1994. "An investigation of electrochemically and chemi-cally polymerized polyindole." *Mater. Rech. Bull.*, vol. 29, p. 1239.
[38] Fajan, A. and Been, B., 2013. "Structural and optical properties of polyindole manganese oxide nanocomposite." *Indian J. ofAdv. In Chem. Sci.*, vol. 2, pp. 95-96.
[39] GiFajan, A., Beribabu, K., Manegand, R., Sinesh, R., Vijaialakchmi, L., Stephen, A., and Narayanan, V., 2013. "Polyindole nanowires: synthesis, characterization and electrochemi.. sensing properties." *Chem . Sci. Trans.*, vol. 2, pp. S13-S16.
[40] Trung, V. Q. and Huyen, D. N., 2009. "Synthesis, properties and application of polyindole/tio 2, asean work shop on advanced materials science and nanotechnology." *J .of Physics, Conferences Seriec*, vol. 187, p. 012058.
[41] Dosio, S. T., Mert, B. D., and Yazicch, B., 2013. "Polyidole top coaton tio2 for corrosion protec-tion of steel." *Corrosion Sci.*, vol. 66,
[42] Zhijiang, C. and Guang, Y., 2010. "Synthesis polyindole and its evaluation for li-ion battery applications." *Synth. Met.*, vol. 160, pp. 1902-1905.
[43] Carollo, A., Equatarone, C., Mustarelli, P., Belloti, F., and Magastris, A., 2006. "Developments of new proton conducting membranes based on different polybenzimidazole structures for fuel cells applications." *Journal of Power Sources*, vol. 160, pp. 175-180.
[44] Glipa, X., El, H., M., Jones, D. J., and Rozi`ere., J. "Synthesisand characterisation of sulfonated polybenzimidazole: a highly conducting proton exchang."
[45] Jones, D. J. and J., R., 2001. "Recent advances in the functionalisation of polybenzimidazole and polyetherketone for fuel cell applications." *Journal of Membrane Science*, vol. 185, pp. 41-58.
[46] Kerres, J. A., 2005. "Blended and cross-linked ionomer membranes for application in membrane fuel cells." *Fuel Cells*, vol. 5, pp. 230-247.
[47] Li, Q. F., He, R. H., Jensen, J. O., and Bierum, N. J., 2004. "PBI based polymer membranes for high temperature fuel cells-preparation, Characterization and fuel cell demonstration." *Fuel Cells*, vol. 4, pp. 147–159.
[48] Liu, C., Khan, S. B., and Lee, M., 2013. "Fuel cell based on novelhyper-branched polybenzimidazole membrane." *Macromolecular Research*, vol. 21, pp. 35-41.
[49] Weinright, J. S., Litt, M. H., Savinel, R. F., Vielstich, W., Lamm, A., and Gasteiger, H. A., 2003. *Handbook of Fuel Cells* vol. 3. John Wiley & Sons: New York, NY, USA.
[50] Lee, J. W., Kim, K., Bahadar, S., Khan, B., Patrick, H., P., Seo, J., and Wonbong, J. W. H., 2014. "Synthesis, Characterization, and thermal and proton conductivity evaluation of 2,5-polybenzimidazole composite membranes." *Journal of Nanomaterials*, p. 460232.
[51] Clearfield, A., 1988. *Inorganic ion exchange materials*. Bocca Raton: CRC Press Fl.
[52] Colon, J. L., Diaz, A., and Clearfeild, A., 2010. "Nanoincapsulation of insulin into zirconium phosphate for oral delivery applications." *Biomacro Molecules*, vol. 9, p. 2465.
[53] Diaz, A., Saxena, V., Gunzalez, J., David, A., Casanas, B., Carpenter, C., Batteas, J. D., Colon, J., Clearfield, A., *et al.*, 2012. "Zirconium phosphate nano-platelets: a novel platform for drug delivery in cancer therapy." *Chem. Commun.*, vol. 48, p. 1754.
[54] Salvado, M. A., Pertierra, P., Tropajo, C., and Garcia, G. R., 2007. "Crystal structure of cerium (iv) bis(hydrogen phosphate derivative." *J. Am. Chem. Soc.*, vol. 129, p. 10970.

[55] Tushato, M., Danjo, M., Baba, Y., Murakom, M., and Nana, H., 1997. "Preparation and chemical properties of a novel layered cerium(iv) phosphate." *Bulletin of Chem.Soc Jap.*, vol. 70, p. 143.

[56] Alberti, G. and Costantino, U., 1974. "Recent progress in the field of synthetic inorganic exchanger having a layered and fibrous structure." *J. Chromatogr.*, vol. 102, p. 5.

[57] Parangi, T., Wani, P., and Chudasama, U., 2012. "Synthesis, characterization and application of cerium phosphate." *Desalination and Water Treatment*, vol. 38, p. 126.

[58] Romano, R. and Alves, O. S., 2005. "Fibrous cerium iv phosphate host of weak and strong lewis bases, inclus." *Phenom. and Macrocyclic*, vol. 51, p. 211.

[59] Casciola, M., Costantino, U., and D´amico, S., 1988. "Ac conductivity of cerium iv phosphate in hydrogen form." *Solid State Ionics*, vol. 28, p. 617.

[60] Shakshooki, S. K., Elejmi, A. A., Hamassi, A. M., El-Akari, F. A., and An, M., N. A., 2014. "Facile synthesis of poly (vinylalcohol)/fibrous cerium phosphate nanocomposite membranes." *Physics and Materials Chemistry*, vol. 2, pp. 1-6.

[61] Metwally, S. S., El-Gammal, B., Ali, H. F., and Abo-EL-Enein, S. A., 2011. "Removal and separation of some radionuclides by poly-acrylamide based ce(iv) phosphate." *Separation Sci. and Tech.*, vol. 46, p. 11.

[62] Alberti, G., Casciola, M., Captani, D., Donnadio, A., Narducci, R., Pica, M., and Sganappa, M. N., 2007. "Novel nafion-zirconium phosphate composite membranes with enhanced stability of proton conductivity." *Electrochemica Acta*, vol. 52, p. 8125.

[63] Nagarale, R. K., Shin, W., and Singh, P. K., 2010. "Progress in ionic organic-inorganic composite membranes for fuel cell application." *Polym. Chem.*, vol. 1, p. 388.

[64] Shakshooki, S. K., Elejmi, A. A., Khalfulla, A. M., and S., E. S., 2010. In *Int. Conf. on Mater. Imperative,Cairo, Egypt , 29/11-2/12*. pp. 49-70.

[65] Yang, Y., Liu, C., and Wen, H., 2009. "Preparation and properties of polyvinyl alcohol / exfoliated α-zirconium phosphate." *Polym. Test.*, vol. 28, p. 185.

[66] Feng, Y., He, W., Zhang, X., Jia, X., and Zhao, H., 2007. "The preparation of nanoparticle zirconium phosphate." *Mater. Letters*, vol. 61, p. 3258.

[67] Bao, C., Gua, Y., Song, L., Lu, H., Yuan, B., and Hu, Y., 2011. "Facile synthesis of poly(vinyl alcohol)/α-titanium phosphate nanocomposite with markedly enhanced properties." *Ind. Eng. Chem. Res.*, vol. 50, p. 11109.

[68] Shakchooki, S. K., El-Akari, F. A., El-Fituri, M. S., and El-Fituri, S. S., 2014. "Fibrous cerium(iv) hydrogen phosphate membrane self supported benzimidazole polymerization agent." *Adv. Mater. Res.*, vol. 856,

[69] Shakshooki, S. K., 2014. "Nano fibrous cerium iv hydrogen phosphate membrane self supportedindole polymerization agent." *J. Chem. Chem. Eng.*, vol. 8, pp. 378-384.

[70] Shakshooki, S. K., El-Akari, F. A., Jangher, A. A., and Hamasi, A. M., 2015. "Facile synthesis of γ-zirconium phosphate-fibrous cerium phosphate/ emeraldine salt nanocomposite membrane." vol. 5, pp. 75-85.

[71] Shakshooki, S. K., Elakari, F. A., M., A., and Shaabani, A. M., 2015. "Exfoliated zirconiumphosphate-fibrous cerium phosphate nanocomposite membrane self supported indole, its co-aniline and co-pyrrole polymerization agent." *American J. of Chem.*, vol. 5, pp. 115-123.

[72] Shakshooki, S. K., Hassan, M. B., and Abdullah, I. M., 2018. "Synthesis and characterization of novel glassy titanium-, zirconium tellurates-fibrous cerium phosphate/ polyaniline, polyindole, polypyrrole, polyaniline-co-polyindole, polyaniline-co-polypyrrole nanocomposite membranes." *American J.of Chem.*, vol. 8, pp. 72-83.